Deformed Relativistic Mean-field Calculations on the Properties of Superheavy Nuclei

Zhongzhou Ren[*,a,b]

[a]*Department of Physics, Nanjing University, Nanjing 210008, P. R. China*
[b]*Center of Theoretical Nuclear Physics, National Laboratory of Heavy-Ion Accelerator at Lanzhou, Lanzhou 730000, P. R. China*

Received: November 13, 2001; In Final Form: November 13, 2001

The structures of the nuclei with the proton number $Z = 106$–110 are systematically investigated using the deformed relativistic mean-field (RMF) theory. The calculated binding energies are in good agreement with experimental ones. The experimental data of α-decay energies are well reproduced by the calculations. Calculations show clearly that a prolate deformation is important for the ground state of these nuclei. The properties of the nuclei on the α-decay chain of ^{269}Mt are predicted.

1. Introduction

It was believed that there is still a long and difficult way to access the superheavy island around $Z = 114$. However the pioneering work of synthesizing elements $Z = 110$–112 by Hofmann et al. at GSI in Germany[1–3] brings a hope to approach the island in near future because the three elements were produced within two years. This speeds up the researches on superheavy nuclei both experimentally and theoretically.[4–7] A breakthrough appeared at Dubna in Russia: the element $Z = 114$ was produced by Oganessian et al.[5,6] in 1999. A year later it was again reported that $Z = 116$ is synthesized at Dubna.[8] At present many big laboratories in the field of nuclear physics focus on the superheavy nuclei. New results are reported such as the synthesis of new nuclide ^{270}Hs in PSI (Ref. 9), ^{270}110 in GSI (Ref. 10), ^{259}Db at Lanzhou.[11]

Theoretically there are some studies on superheavy nuclei based on the self-consistent mean-field models or macrosocpic-microscopic mass models.[13–24] The Frankfurt group tested the relativistic mean-field (RMF) model for a known nucleus ^{264}Hs (Ref. 13). Ćwiok et al. investigated the ground state properties of the α-decay chain ^{289}114 within the framework of the Skyrme-Hartree-Fock-Bogoliubov model.[14] Ren and Toki systematically calculated the properties of superheavy nuclei on the decay chain of $Z = 110$–112 and $Z = 114$ in the RMF model.[19] Shape coexistence is predicted in the ground state of superheavy nuclei and deformation can be an important cause for the stability of superheavy nuclei based on a constraint RMF calculation.[19]

In this paper we study the properties of nuclei on the isotope chain $Z = 108$, 109, and 110. Now these nuclei are possibly produced in many laboratories. ^{270}Hs and ^{270}110 have been synthesized in PSI and GSI, respectively.[9,10] After ^{259}Db is observed at Lanzhou in China,[11] it is planned to investigated the properties of nuclei with $Z = 108$ and $Z = 109$ experimentally soon.[12] The nuclei in this range also bridge the gap from the known actinide series to the unknown superheavy nuclei. Especially there are some indications that deformations may be important in this range.

This paper is organized in the following way. Section 2 is the formalism of the RMF model. The numerical results and discussions are given in sect. 3. Section 4 is a summary.

2. The Formalism of the Relativistic Mean-field Theory

In the RMF approach, we start from the local Lagrangian density for interacting nucleons, σ, ω, and ρ mesons, and photons,[25–35]

$$\begin{aligned}\mathcal{L} \;=\; & \overline{\Psi}(i\gamma^\mu\partial_\mu - M)\Psi - g_\sigma\overline{\Psi}\sigma\Psi - g_\omega\overline{\Psi}\gamma^\mu\omega_\mu\Psi \\ & - g_\rho\overline{\Psi}\gamma^\mu\rho^a_\mu\tau^a\Psi + \frac{1}{2}\partial^\mu\sigma\partial_\mu\sigma - \frac{1}{2}m^2_\sigma\sigma^2 - \frac{1}{3}g_2\sigma^3 \\ & - \frac{1}{4}g_3\sigma^4 + \frac{1}{4}c_3(\omega_\mu\omega^\mu)^2 - \frac{1}{4}\Omega^{\mu\nu}\Omega_{\mu\nu} + \frac{1}{2}m^2_\omega\omega^\mu\omega_\mu \\ & - \frac{1}{4}R^{a\mu\nu}\cdot R^a_{\mu\nu} + \frac{1}{2}m^2_\rho\rho^{a\mu}\cdot\rho^a_\mu - \frac{1}{4}F^{\mu\nu}F_{\mu\nu} \\ & - e\overline{\Psi}\gamma^\mu A^\mu\frac{1}{2}(1-\tau^3)\Psi \end{aligned} \tag{1}$$

with

$$\Omega^{\mu\nu} = \partial^\mu\omega^\nu - \partial^\nu\omega^\mu, \tag{2}$$
$$R^{a\mu\nu} = \partial^\mu\rho^{a\nu} - \partial^\nu\rho^{a\mu}, \tag{3}$$
$$F^{\mu\nu} = \partial^\mu A^\nu - \partial^\nu A^\mu, \tag{4}$$

where the meson fields are denoted by σ, ω_μ, and ρ^a_μ, and their masses are denoted by m_σ, m_ω, and m_ρ, respectively. The nucleon field and rest mass are denoted by Ψ and M. A_μ is the photon field which is responsible for the electromagnetic interaction, $e^2/4\pi = 1/137$. The effective strengths of the coupling between the mesons and nucleons are, respectively, g_σ, g_ω, and g_ρ. g_2 and g_3 are the nonlinear coupling strengths of the σ meson. c_3 is the self-coupling term of the ω field. The isospin Pauli matrices are written as τ^a, τ^3 being the third component of τ^a.

The equations of motion for the fields are easily obtained from the variational principle.[19,25–29] In order to describe the ground state properties of nuclei we need static solution of the above Lagrangian. For this case the meson field and photon fields are assumed to be classical fields and they are time independent (c-numbers). The nucleons move in classical fields as independent particles (mean-field approximations). The Dirac field operator can be expanded in terms of single particle wave functions $\Psi = \sum_i \phi_i a_i$ where a_i is a particle creation operator[25,26] and ϕ_i is the single particle wave function. For actual calculations, we omit the contribution of the Fermi-sea under no-sea approximations. The sum on single particles states runs on physical bound states, i.e. the occupied shell model states. Symmetries will simplify the calculations considerably. Time reversal symmetry is used and therefore the spacial vector components for ω_μ, ρ^a_μ, and A_μ are zero. Charge conservation guarantees that only the third-component of the isovector field (ρ^0_0) survives.[25–28] We denote simply ρ^0_0 as ρ_0. Finally we have the following Dirac equations for nucleons and the Klein-Gordon equations for meson fields (for details: see References 25–28):

$$[-i\boldsymbol{\alpha}\bigtriangledown + \beta M^*(\mathbf{r}) + V(\mathbf{r})]\phi_i(\mathbf{r}) = \varepsilon_i\phi_i(\mathrm{r}), \tag{5}$$

where the effective mass $M^*(\mathbf{r}) = M + g_\sigma\sigma(\mathrm{r})$. The potential

*E-mail: zren@nju.edu.cn; zren99@yahoo.com.
FAX: +86-25-3326028.

Published on Web 6/30/2002

TABLE 1: The ground state properties of even-even superheavy nuclei with $Z = 108$. The TMA force is inputted in the deformed RMF calculation. The last two columns are the experimental data of the α-decay energy and the total binding energy.

Nuclei	$B_{\text{the.}}$ / MeV	β_n	β_p	R_n	R_p	Q_α(the.)	Q_α(exp.)	$B_{\text{exp.}}$ / MeV
^{256}Hs	1864.99	0.26	0.27	6.15	6.04	10.99		
^{258}Hs	1882.16	0.25	0.26	6.16	6.05	10.58		
^{260}Hs	1899.03	0.25	0.26	6.18	6.05	9.96		
^{262}Hs	1915.26	0.25	0.25	6.21	6.06	9.59		
^{264}Hs	1930.17	0.24	0.25	6.23	6.07	9.98	10.54	1926.72
^{266}Hs	1944.46	0.24	0.24	6.24	6.08	9.74	10.18	
^{268}Hs	1958.42	0.22	0.23	6.26	6.09	9.14		
^{270}Hs	1971.80	0.22	0.22	6.28	6.10	8.90	9.30	
^{272}Hs	1984.60	0.21	0.22	6.30	6.11	8.77		
^{274}Hs	1996.62	0.20	0.20	6.32	6.12	8.88		
^{276}Hs	2007.73	0.19	0.20	6.34	6.13	9.26		

TABLE 2: The ground state properties of even-even superheavy nuclei with $Z = 108$. The NLZ2 force is inputted in the deformed RMF calculation. The last two columns are the experimental data of the α-decay energy and the total binding energy.

Nuclei	$B_{\text{the.}}$ / MeV	β_n	β_p	R_n	R_p	Q_α(the.)	Q_α(exp.)	$B_{\text{exp.}}$ / MeV
^{256}Hs	1862.85	0.30	0.32	6.27	6.13	10.72		
^{258}Hs	1879.66	0.30	0.31	6.31	6.15	11.11		
^{260}Hs	1895.90	0.29	0.30	6.31	6.15	11.15		
^{262}Hs	1911.48	0.28	0.29	6.33	6.16	11.08		
^{264}Hs	1926.63	0.28	0.29	6.35	6.17	10.68	10.54	1926.72
^{266}Hs	1941.35	0.28	0.29	6.38	6.18	10.30	10.18	
^{268}Hs	1955.59	0.27	0.28	6.40	6.19	9.96		
^{270}Hs	1969.22	0.27	0.28	6.42	6.20	9.55	9.30	
^{272}Hs	1981.03	0.26	0.27	6.45	6.21	10.26		
^{274}Hs	1992.08	0.25	0.26	6.47	6.22	10.15		
^{276}Hs	2003.31	0.20	0.22	6.48	6.22	9.10		

$V(\mathbf{r})$ is a timelike component of a Lorentz vector,

$$V(\mathbf{r}) = g_\omega \omega_0(\mathrm{r}) + g_\rho \tau^a \rho_0^a(\mathrm{r}) + e((1-\tau^3)/2)A_0(\mathrm{r}), \tag{6}$$

$$(-\triangle + m_\sigma^2)\sigma(\mathbf{r}) = -g_\sigma \rho_s(\mathrm{r}) - g_2\sigma^2(\mathrm{r}) - g_3\sigma^3(\mathrm{r}), \tag{7}$$

$$(-\triangle + m_\omega^2)\omega_0(\mathbf{r}) = g_\omega \rho_v(\mathrm{r}) - c_3\omega_0^3(\mathrm{r}), \tag{8}$$

$$(-\triangle + m_\rho^2)\rho_0(\mathbf{r}) = g_\rho \rho_3(\mathrm{r}), \tag{9}$$

$$-\triangle A_0(\mathbf{r}) = e\rho_p(\mathrm{r}), \tag{10}$$

where ρ_s, ρ_v, and ρ_p are, respectively, the densities of scalar, baryon, and proton. ρ_3 is the difference between the neutron and proton densities. They will be c-numbers by taking expectation values. Their expressions are as follows,

$$\rho_s(\mathbf{r}) = \sum_{i=1}^{A} \overline{\phi_i}(\mathrm{r})\phi_i(\mathrm{r}), \tag{11}$$

$$\rho_v(\mathbf{r}) = \sum_{i=1}^{A} \phi_i^+(\mathrm{r})\phi_i(\mathrm{r}), \tag{12}$$

$$\rho_3(\mathbf{r}) = \sum_{i=1}^{A} \phi_i^+(\mathrm{r})\tau^3\phi_i(\mathrm{r}), \tag{13}$$

$$\rho_p(\mathbf{r}) = \sum_{i=1}^{A} \phi_i^+(\mathrm{r})((1-\tau^3)/2)\phi_i(\mathrm{r}). \tag{14}$$

Now we have a set of coupled equations for mesons and nucleons and they will be solved consistently by the iteration. After the final solution is obtained, we can calculate the binding energies, root-mean-square radii of proton and neutron density distributions, single particle levels, and quadrupole deformation. An axial deformation is assumed in our calculations for superheavy nuclei. The details of numerical calculations are described in References 19, 25–28.

3. Numerical Results and Discussions

We carry out RMF calculations with two typical sets of force parameters, TMA[19] and NLZ2[15,20] where the method of the harmonic basis expansion[19,27,29–31,33] is used. The number of bases is chosen as $N_f = N_b = 20$. This space is enough for the calculations. The inputs of pairing gaps are $\Delta_n = \Delta_p = 11.2/\sqrt{A}$ MeV. An axial deformation is assumed in calculations. For the details of calculations please see relevant publications.[19,27,29,31]

At first let us focus on the global behaviour of the RMF model. We calculate the average binding energy of nucleons (B/A) for $Z = 98$, 100, 102, 104, 106, and 108 isotopes and draw the variation of average binding energy with nuclei in Figure 1. In Figure 1, the X-axis is just used for the sequence of different nuclei. We choose four even-even nuclei for every isotope where the experimental data are available for many of them.[36] The theoretical results are denoted by RMF1.dat and RMF0.dat where they correspond to the results of TMA and NLZ2, respectively. They are connected by solid lines. The experimental average binding energy[36] is denoted by EXP.dat. It is seen from Figure 1

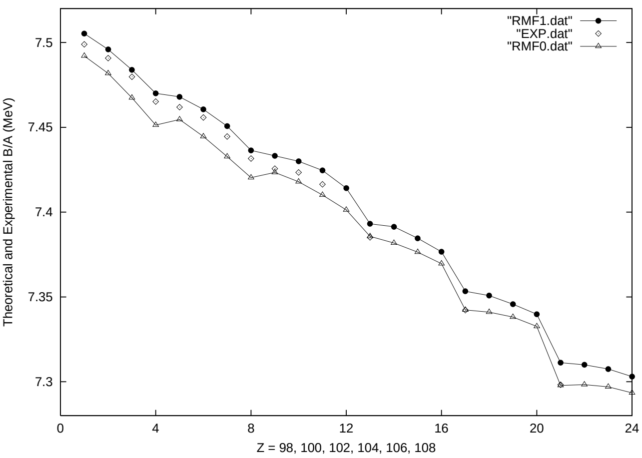

Figure 1. The comparison of theoretical and experimental average binding energy of nucleons for nuclei with $Z = 98$, 100, 102, 104, 106, and 108. For every isotope the results of four nuclei are shown. This includes the present data of binding energy for even-even nuclei in these isotopes. It is interesting to note that the experimental data lie between two sets of the RMF results. The TMA force and NLZ2 force are used in calculations.

TABLE 3: The ground state properties of even-even superheavy nuclei with $Z = 110$. The TMA force is inputted in the deformed RMF calculation. The last column is the experimental data of the α-decay energy.

Nuclei	$B_{\mathrm{the.}}$ / MeV	β_n	β_p	R_n	R_p	Q_α(the.)	T_α(the.)	Q_α(exp.)
^{268}110	1946.70	0.23	0.24	6.25	6.11	11.77	4.37 μs	
^{270}110	1961.39	0.22	0.22	6.26	6.11	11.37	33.6 μs	10.97
^{272}110	1975.66	0.21	0.22	6.28	6.12	11.06	176 μs	
^{274}110	1989.43	0.20	0.21	6.30	6.13	10.67	1.57 ms	
^{276}110	2002.54	0.19	0.20	6.32	6.13	10.36	9.71 ms	
^{278}110	2014.56	0.18	0.19	6.34	6.14	10.36	9.71 ms	
^{280}110	2025.95	0.17	0.18	6.36	6.15	10.08	54.2 ms	

TABLE 4: The ground state properties of even-even superheavy nuclei with $Z = 110$. The NLZ2 force is inputted in the deformed RMF calculation. The last column is the experimental data of the α-decay energy.

Nuclei	$B_{\mathrm{the.}}$ / MeV	β_n	β_p	R_n	R_p	Q_α(the.)	T_α(the.)	Q_α(exp.)
^{268}110	1943.91	0.26	0.27	6.37	6.20	11.02	219 μs	
^{270}110	1958.87	0.26	0.26	6.40	6.21	10.78	835 μs	10.97
^{272}110	1973.31	0.25	0.26	6.42	6.22	10.58	2.63 ms	
^{274}110	1986.07	0.24	0.24	6.44	6.22	11.45	22.2 μs	
^{276}110	1998.68	0.21	0.22	6.45	6.23	10.65	1.76 ms	
^{278}110	2010.86	0.20	0.21	6.47	6.24	9.52	2.16 s	
^{280}110	2022.80	0.18	0.19	6.49	6.25	8.81	361 s	

that the experimental points lie between two theoretical curves. Therefore the RMF model can reliably limit the data in a very narrow range. This can be useful for future experimental study.

Secondly we discuss in detail the theoretical results. The variation of the total binding energy with nucleon number for $Z = 106$ isotopes are given in Figure 2. The two sets of theoretical results with TMA and NLZ2 are represented by two curves (Z106RMF1.dat and Z106RMF0.dat). For this isotope chain, only the binding energy of ^{260}Sg is measured and it is plotted by a point (Z106EXP.dat). The experimental datum[36] is between two curves. The difference between two sets of theoretical results is very small and this is a good indication for the stability and reliability of the model in this mass range.

The theoretical results of $Z = 108$ isotopes with TMA and NLZ2 are listed in Tables 1 and 2, respectively. In Tables 1 and 2, the first column is for nuclei. $B_{\mathrm{the.}}$ is the theoretical binding energy, whereas R_p and R_n are the root-mean-square radii for the proton- and neutron-density distributions, respectively. The symbols β_n and β_p in Tables 1 and 2 denote the quadrupole deformations of neutrons and protons, respectively. Further, the symbols Q_α(the.) and Q_α(exp.) are used for the calculated α-decay energies and the experimental ones. The experimental binding energies are obtained from the nuclear mass table[36] and the experimental α-decay energies can be deduced accordingly. They are listed in the last two columns for comparisons. The binding energies of $Z = 106$ in Figure 2 are inputted for the calculation of α-decay energies of $Z = 108$.

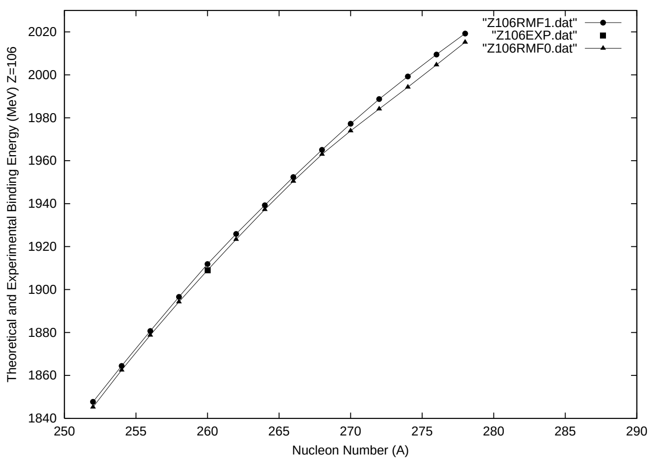

Figure 2. The variation of the total binding energy of $Z = 106$ isotopes with nucleon number (A). The two sets of theoretical results are connected by solid lines.

It is seen from Table 1 that the theoretical decay energies are very close to the experimental data. The average difference between the theoretical binding energy and experimental one is approximately 0.4 MeV. This shows that the RMF model can give a reliable result for the decay energy. The maximum difference for the binding energy of this mass range is 3.45 MeV for ^{264}Hs. It corresponds to a relative difference 0.2%. This is very close to the predicting limit of the RMF model for the binding energy of a nucleus.

Table 2 is the RMF results of $Z = 108$ with NLZ2. The theoretical decay energy is very close to the data. The binding energy agrees well with the experimental datum. If we compare Tables 1 and 2 together, we find both results are very close. The RMF model with TMA overestimates very slightly the data of binding energy and that with NLZ2 underestimate a little the data. Both of them predict there are prolate deformation in these nuclei. The parameter of quadrupole deformation (β_n and β_p) is approximately 0.2–0.3. A constraint RMF calculation with NLZ2 is carried out for the nucleus ^{270}Hs. The energy surface of ^{270}Hs with the variation of quadrupole deformation is plotted in Figure 3. Here the number of the bases is chosen as $N_f = N_b = 18$. It is seen clearly that there exists a minimum at $\beta_2 = 0.27$. This corresponds to the ground state of ^{270}Hs in Table 2.

The variation of decay energy with nucleon number are drawn in Figure 4. The experimental points are between two sets of

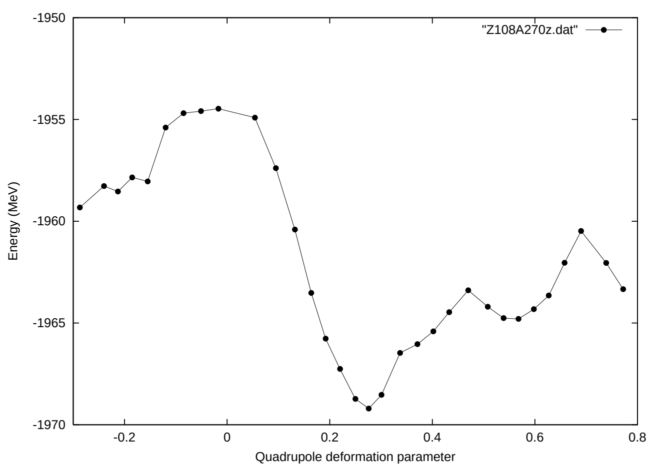

Figure 3. The energy surface of ^{270}Hs. This is the variation of the ground state energy with the quadrupole deformation. The points are numerical results and they are connected by solid lines. A mimimum appears at the deformation parameter 0.27 and it corresponds to the deformation of the ground state.

TABLE 5: The binding energies, deformations, nuclear radii, α-decay energies, and the lifetimes of nuclei on the α-decay chain ^{269}Mt. The input pairing gaps: $\Delta_p = \Delta_n = 11.2/\sqrt{A}$ MeV. The TMA force is used.

Nuclei	B / MeV	β_n	β_p	R_n	R_p	Q_α	T_α
^{269}Mt	1960.17	0.22	0.23	6.26	6.10	10.21	68.8 ms
^{265}Bh	1942.08	0.23	0.24	6.24	6.07	9.41	2.56 s
^{261}Db	1923.19	0.26	0.27	6.23	6.05	9.14	3.33 s
^{257}Lr	1904.03	0.26	0.27	6.20	6.01	8.12	1.28×10^3 s
^{253}Md	1883.85	0.26	0.27	6.17	5.98	7.68	8.4×10^3 s
^{249}Es	1863.23	0.26	0.27	6.14	5.94	6.91	1.53×10^6 s
^{245}Bk	1841.84	0.27	0.28	6.12	5.91		

TABLE 6: The binding energies, deformations, nuclear radii, α-decay energies, and the lifetimes of nuclei on the α-decay chain of ^{269}Mt. The input pairing gaps: $\Delta_p = \Delta_n = 11.2/\sqrt{A}$ MeV. The NLZ2 force is used.

Nuclei	B / MeV	β_n	β_p	R_n	R_p	Q_α	T_α
^{269}Mt	1957.41	0.27	0.28	6.40	6.20	10.45	16.4 ms
^{265}Bh	1939.56	0.28	0.30	6.38	6.17	9.63	595 ms
^{261}Db	1920.89	0.29	0.31	6.36	6.14	8.44	568 s
^{257}Lr	1901.03	0.30	0.31	6.33	6.10	7.51	2.4×10^5 s
^{253}Md	1880.24	0.30	0.31	6.30	6.07	7.78	3.58×10^3 s
^{249}Es	1859.72	0.31	0.31	6.27	6.03	7.58	3.16×10^3 s
^{245}Bk	1839.00	0.31	0.32	6.25	6.00		

theoretical results. The sudden increase of the decay energy on one curve beyond $A = 270$ (NLZ2) is a signature of the deformed shell closure for $Z = 108$ and $N = 162$. We get a similar result from the single particle levels for NLZ2. This effect is not very evident for TMA. We expect that there is a deformed shell closure for $Z = 108$ and $N = 162$ but its strength is between the two theoretical results. We should notice that the shell gap in superheavy nuclei is not large as compared with that around ^{208}Pb. Maybe the shell gap in superheavy nuclei can be only seen in the decay energy or lifetime. This can be different from that around ^{208}Pb where many quantities demonstrate the existence of a large gap.

The numerical results for $Z = 110$ isotopes are listed in Tables 3 and 4. The α-decay energies of this isotope chain are plotted in Figure 5. In order to compare with future experiments, we also list the theoretical lifetime of these nuclei in Tables 3 and 4. The theoretical lifetime T_α(the.) is calculated according to the Viola-Seaborg formula on α decays,[21,37]

$$\log(T_\alpha) = (aZ+b)(Q_\alpha)^{-1/2} + (cZ+d) + h_{log}\,, \qquad (15)$$

where T_α is given in second and Q_α in MeV, and Z is the proton number of the parent nucleus. This formula is usually used to estimate the lifetime of α decays by the decay energies.[21,37] The constants in this expression have been determined as $a = 1.66175$, $b = -8.5166$, $c = -0.20228$, $d = -33.9069$, $h_{log} = 0.0$ for even-even nuclei. These values are obtained by fitting the experimental data of middle and heavy nuclei.[21,22,24,37]

It is concluded from Tables 3 and 4 that there is prolate deformation for the ground state of these nuclei. The binding energies for two sets of theoretical results are close. It is expected the experimental data of binding energy will be between two sets of theoretical results. As a good estimate on the binding energy and α-decay energy of unknown nuclei, we suggest to choose the average value of two sets of theoretical results. The experimental data should be very close to this average value. On the lifetime, there is a difficulty to predict it in a good precision. But it is very important for experimental physicists to adjust the detectors to observe a new element or a new nuclide. We also suggest to take the average of two theoretical values as an estimated value. But this average value on lifetime should not be chosen as a sum of two values divided by two. It should be an average with an exponential weight. For example, if one theoretical value is 10 ms (10^1) and another theoretical value is 1000 ms (10^3), people should choose 100 ms (10^2) as an estimate value of measurements. It is stressed again that it is difficult to reproduce the experimental lifetime well by theory. The difference with 100 times between theory and experiment should be considered very well.

It is seen from Figure 5 that the experimental datum of decay energy is between two theoretical values. There is a strong deformed shell closure at $N = 162$ for NLZ2 (Z110RMF0.dat).

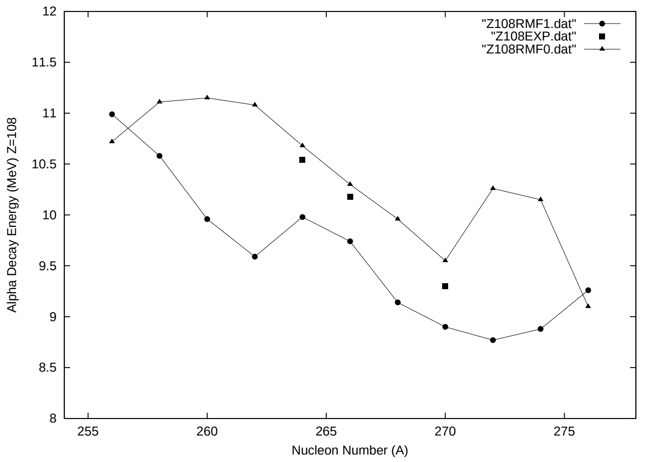

Figure 4. The variation of the α-decay energy of $Z = 108$ isotopes with nucleon number (A). The two sets of theoretical results are connected by solid lines. It is expected that experimental data lie between two theoretical results.

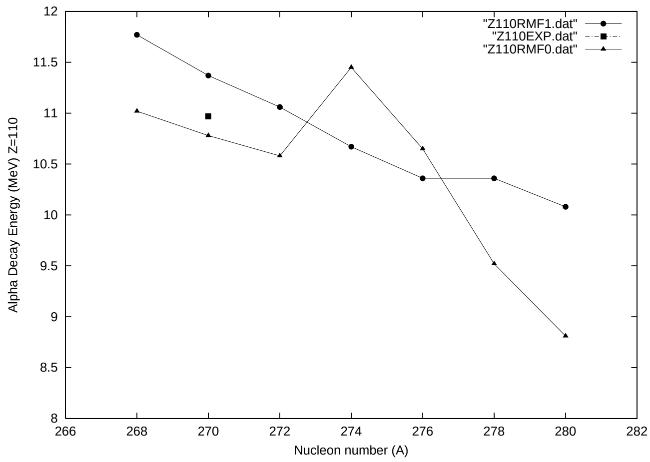

Figure 5. The variation of the α-decay energy of $Z = 110$ isotopes with nucleon number (A). The two sets of theoretical results are connected by solid lines. It is expected that experimental data lie between two theoretical results.

It leads to a sudden increase of decay energy beyond $N = 162$. This effect is not so evident for TMA (Z110RMF1.dat).

Finally let us make a prediction for planned experiments at Lanzhou in China. After the nuclide ^{259}Db is identified at Lanzhou in China,[11] it is planned to synthesize new nuclide with $Z = 108$ (Hs) or $Z = 109$ (Mt) soon.[12] The properties of $Z = 108$ isotopes have been listed in Tables 1 and 2. Here we give the theoretical prediction on the α-decay chain of ^{269}Mt in Tables 5 and 6. It is nice to see that the α-decay energy and the lifetime of ^{269}Mt and ^{265}Bh from two sets of forces are very close. The experimental data can be between them. Although there is a difference of decay energy and lifetime for low mass nuclei in Tables 5 and 6, this is not important because the α-decay chain is generally not so long. The fission can appear in the low mass range.

4. Summary

We have investigated the structure of nuclei with proton number $Z = 106$–110 in the RMF model. The theoretical binding energy of the RMF model agrees well with the available data. The calculations set an upper limit and a lower limit for the binding energy based on the comparison with present data. This is useful for the good estimate of the binding energy, decay properties on unknown nuclei. The RMF results show that there is prolate deformation in these nuclei. There may exist a deformed shell closure for $Z = 108$ and $N = 162$. The prediction for future experiments such as the properties of nuclei on the α-decay chain of ^{269}Mt is made.

Acknowledgments. Z. REN thanks Profs. T. Otsuka, H. Toki, W. Q. Shen, H. Q. Zhang, Z. Qin, Z. G. Gan, J. S. Guo for kindly communicating him new progress related to superheavy nuclei. This work is supported by the National Natural Science Foundation of China (10125521), the 973 National Major State Basic Research and Development of China (G2000077400), and by the CAS Knowlidge Innovation Project No. KJCX2-SW-N02.

References

(1) S. Hofmann, V. Ninov, F. P. Heßberger, P. Armbruster, H. Folger, G. Münzenberg, H. J. Schött, A. G. Popeko, A. V. Yeremin, A. N. Andreyev, S. Saro, R. Janik, and M. Leino, Z. Phys. A **350**, 277 (1995).
(2) S. Hofmann, V. Ninov, F. P. Heßberger, P. Armbruster, H. Folger, G. Münzenberg, H. J. Schött, A. G. Popeko, A. V. Yeremin, A. N. Andreyev, S. Saro, R. Janik, and M. S. Leino, Z. Phys. A **350**, 281 (1995).
(3) S. Hofmann, V. Ninov, F. P. Heßberger, P. Armbruster, H. Folger, G. Münzenberg, H. J. Schött, A. G. Popeko, A. V. Yeremin, S. Saro, R. Janik, and M. Leino, Z. Phys. A **354**, 229 (1996).
(4) S. Hofmann, Rep. Prog. Phys. **61**, 639 (1998).
(5) Yu. Ts. Oganessian, A. V. Yeremin, A. G. Popeko, S. L. Bogomolov, G. V. Buklanov, M. L. Chelnokov, V. I. Chepigin, B. N. Gikal, V. A. Gorshkov, G. G. Gulbekian, M. G. Itkis, A. P. Kabachenko, A. Y. Lavrentev, O. N. Malyshev, J. Rohä, R. N. Sagaidak, S. Hofmann, S. Saro, G. Giardina, and K. Morita, Nature (London) **400**, 242 (1999).
(6) Yu. Ts. Oganessian, V. K. Utyonkov, Yu. V. Lobanov, F. Sh. Abdullin, A. N. Polyakov, I. V. Shirokovsky, Yu. S. Tsyganov, G. G. Gulbekian, S. L. Bogomolov, B. N. Gikal, A. N. Mezentsev, S. Iliev, V. G. Subbotin, A. M. Sukhov, G. V. Buklanov, K. Subotic, and M. G. Itkis, Phys. Rev. Lett. **83**, 3154 (1999).
(7) Yu. Ts. Oganessian, V. K. Utyonkov, Yu. V. Lobanov, F. Sh. Abdullin, A. N. Polyakov, I. V. Shirokovsky, Yu. S. Tsyganov, G. G. Gulbekian, S. L. Bogomolov, B. N. Gikal, A. N. Mezentsev, S. Iliev, V. G. Subbotin, A. M. Sukhov, O. V. Ivanov, G. V. Buklanov, K. Subotic, M. G. Itkis, K. J. Moody, J. F. Wild, N. J. Stoyer, M. A. Stoyer, and R. W. Lougheed, Phys. Rev. C **62**, 041604(R) (2000).
(8) Yu. Ts. Oganessian, V. K. Utyonkov, Yu. V. Lobanov, F. Sh. Abdullin, A. N. Polyakov, I. V. Shirokovsky, Yu. S. Tsyganov, G. G. Gulbekian, S. L. Bogomolov, B. N. Gikal, A. N. Mezentsev, S. Iliev, V. G. Subbotin, A. M. Sukhov, O. V. Ivanov, G. V. Buklanov, K. Subotic, M. G. Itkis, K. J. Moody, J. F. Wild, N. J. Stoyer, M. A. Stoyer, R. W. Lougheed, C. A. Laue, Ye. A. Karelin, and A. N. Tatarinov, Phys. Rev. C **63**, 011301(R) (2001).
(9) A. Türler, *Evidence for the New Nuclide ^{270}Hs* (private communication, submitted to Phys. Rev. Lett.).
(10) S. Hofmann, F. P. Heßberger, D. Ackermann, S. Antalic, P. Cagarda, S. Ćwiok, B. Kindler, J. Kojouharova, B. Lommel, R. Mann, G. Münzenberg, A. G. Popeko, S. Saro, H. J. Schött, and A. V. Yeremin, Eur. Phys. J. A **10**, 5 (2001).
(11) Z. G. Gan, Z. Qin, H. M. Fan, X. G. Lei, Y. B. Xu, J. J. He, H. Y. Liu, X. L. Wu, J. S. Guo, X. H. Zhou, S. G. Yuan, and G. M. Jin, Eur. Phys. J. A **10**, 21 (2001).
(12) Z. Qin, Z. G. Gan, and J. S. Guo (private communications, 2001).
(13) K. Rutz, M. Bender, T. Buervenich, T. Schilling, P. G. Reinhard, J. A. Maruhn, and W. Greiner, Phys. Rev. C **56**, 238 (1997).
(14) S. Ćwiok, W. Nazarewicz, and P. H. Heenen, Phys. Rev. Lett. **83**, 1108 (1999).
(15) M. Bender, Phys. Rev. C **61**, 031302 (2000).
(16) W. Q. Shen, J. Albinski, A. Gobbi, S. Gralla, K. D. Hildenbrand, N. Herrmann, J. Kuzminski, W. F. J. Müller, H. Stelzer, J. Tōke, B. B. Back, S. Bjørnholm, and S. P. Sørensen, Phys. Rev. C **36**, 115 (1987).
(17) H. Q. Zhang, Nucl. Phys. Rev. **16**, 192 (1999) (in Chinese).
(18) Zhongzhou Ren, Z. Y. Zhu, Y. H. Cai, G. O. Xu, J. Phys. G **22**, 1739 (1996).
(19) Zhongzhou Ren and H. Toki, Nucl. Phys. A **689**, 691 (2001).
(20) M. Bender, K. Rutz, P. G. Reinhard, J. A. Maruhn, and W. Greiner, Phys. Rev. C **60**, 034304 (1999).
(21) P. Möller, J. R. Nix, and K. L. Kratz, At. Data Nucl. Data Tables **66**, 131 (1997).
(22) R. Smolanczuk, Phys. Rev. C **59**, 2634 (1999).
(23) I. Muntian, Z. Patyk, and A. Sobiczwski, Phys. Lett. B **500**, 241 (2001).
(24) W. D. Myers and W. J. Swiatecki, Phys. Rev. C **58**, 3668 (1998).
(25) B. D. Serot and J. D. Walecka, Adv. Nucl. Phys. **16**, 1 (1986).
(26) P. G. Reinhard, D. J. Dean, W. Nazarewicz, J. Dobaczewski, J. A. Maruhn, and M. R. Strayer, Phys. Rev. C **60**, 014316 (1999).
(27) Y. K. Gambhir, P. Ring, and A. Thimet, Ann. Phys. (N.Y.) **198**, 132 (1990).
(28) S. Marcos, N. Van Giai, and L. N. Savushkin, Nucl. Phys. A **549**, 143 (1992).
(29) D. Hirata, H. Toki, I. Tanihata, and P. Ring, Phys. Lett. B **314**, 168 (1993).
(30) Zhongzhou Ren, Z. Y. Zhu, Y. H. Cai, and Gongou Xu, Phys. Lett. B **380**, 241 (1996).
(31) T. R. Werner, J. A. Sheikh, W. Nazarewicz, M. R. Strayer, A. S. Umar, and M. Misu, Phys. Lett. B **333**, 303 (1994).
(32) Zhongzhou Ren, Amand Faessler, and A. Bobyk, Phys. Rev. C **57**, 2752 (1998).
(33) B. Q. Chen, Z. Y. Ma, F. Gruemmer, and S. Krewald, Phys. Lett. B **455**, 13 (1999).
(34) G. A. Lalazissis, M. M. Sharma, P. Ring, and Y. K. Gambhir, Nucl. Phys. A **608**, 202 (1996).
(35) S. K. Patra, C. L. Wu, C. R. Praharaj, and R. K. Gupta,

Nucl. Phys. A **651**, 117 (1999).
(36) G. Audi, O. Bersilion, J. Blachot, and A. H. Wapstra, Nucl. Phys. A **624**, 1 (1997).
(37) V. E. Viola, Jr. and G. T. Seaborg, J. Inorg. Nucl. Chem. **28**, 741 (1966).